Inhibition of miR-25 aggravates diabetic peripheral neuropathy

Yanzhuo Zhang, Chunyu Song, Jing Liu, Yonghong Bi and Hao Li

The hyperglycemia-induced enhanced oxidative stress is a key factor of diabetic peripheral neuropathy implicated in the pathogenesis of diabetic neuropathy, and microRNA may be involved, playing promotion or protection roles. In this study, we aimed to investigate the function of miR-25 during the development of oxidative/nitrative stress and in subsequent neurological problems. We detected the oxidative stress effects and expression of miR-25 on sciatic nerves from db/db diabetic model mice and analyzed the expression of related genes by qPCR and Western blotting. Interestingly, we observed increased reactive oxygen species (ROS) and Nox4 expression in db/db mice accompanied with reduced miR-25. MiR-25 inhibitor treatment increased nicotinamide adenine dinucleotide phosphate activity in Schwann cells, whereas miR-25 precursor overexpression led to opposite results. MiR-25 precursor reduced the activation of protein kinase C and decreased Nox4 expression at both mRNA and protein levels. Advanced glycation endproducts (AGEs) and the receptor for advanced glycation endproducts (RAGE) were increased in the serum and in the peripheral nerves obtained from diabetic mice, and miR-25 inhibitor treatment in Schwann cells from wt mice led to the same effect. However, miR-25 precursor transfection reduced AGEs and RAGE, and further reduced inflammatory factors that contribute to the pathological process of peripheral nerves. These findings, for the first time, indicate that miR-25 acts as a protection factor in diabetic neuropathy by downregulating AGE–RAGE and reducing nicotinamide adenine dinucleotide phosphate oxidase. miR-25 reduced protein kinase C-α phosphorylation to produce less reactive oxygen species in diabetic peripheral nerves, and therefore it played an important role in the regulation of oxidative/nitrative stress and in consequent neurological dysfunction. *NeuroReport* 29:945–953 Copyright © 2018 The Author(s). Published by Wolters Kluwer Health, Inc.

Department of Anesthesiology, China and Heilongjiang Key Laboratory for Anesthesia and Critical Care, The Second Affiliated Hospital of Harbin Medical University, Harbin, People's Republic of China

Correspondence to Yanzhuo Zhang, MD, Department of Anesthesiology, China and Heilongjiang Key Laboratory for Anesthesia and Critical Care, The Second Affiliated Hospital of Harbin Medical University, Harbin 150086, China
Tel: + 86 177 4512 6625; e-mail: zhangyanzhuowwm@163.com

Introduction

Diabetes mellitus is a metabolic disorder featured by chronic hyperglycemia associated with impaired insulin production and/or secretion. Diabetes has become a global health problem affecting people all over the world. As predicted, the diabetic population worldwide will rise to 592 million by the year 2035 [1]. It is reported that there will be more than a 40% increase in the developed countries and a 170% plus increase in the developing countries in diabetes by 2030 [2]. Diabetes may cause multiple complications associated with microvascular problems, among which diabetic neuropathy (DN), with a prevalence of 50–60%, is a major one [3]. The clinical manifestations of DN include numbness, burning and tingling sensation, and neuralgia [4]. Multiple researches have indicated that oxidative stress, induced by hyperglycemia and subsequent increased reactive oxygen species (ROS), is the major cause leading to the occurrence and development of DN [5–12]. Hyperglycemia would trigger activation of downstream pathways such as advanced glycation end products (AGEs) and polyol pathways to mediate cellular damage [13]. Generation of superoxide from mitochondrial electron transport chain is known to increase nicotinamide adenine dinucleotide phosphate (NADPH) oxidase activation via phosphorylation of protein kinase C (PKC-α), which is downstream of the AGE–receptor for advanced glycation endproducts(RAGE) for AGE interaction in superoxide production [14,15]. Hyperglycemia and consequent excess stress, AGEs, PKC, and mitogen-activated protein kinases could lead to increased expression of key inflammatory factors [16–18], which play a major role in the progression of DN. These signaling pathways prolong the effect period of superoxide anions and amplify the pathogenesis damages.

miRNAs are evolutionarily conserved, short noncoding RNAs with a length of 20–25 nucleotides, participating in multiple cell activities including proliferation, differentiation, apoptosis, and post-transcriptional gene modulation. A previous study revealed that the expression of miR-25, which targeted the 3′ untranslated region of Nox4 mRNA,

was reduced in the kidney of diabetic model rats, leading to the activation of AGEs and RAGE pathway by dysregulation of Nox4 mRNA level [19]. Multiple studies found that miR-25 modulated the proliferation of neural stem cells and neural progenitors, indicating that miR-25 may play a role in maintaining the normal structure and function of the nervous system [20]. This study attempts to evaluate the effects of miR-25 on DN pathogenesis and to reveal the underlying mechanisms. Here, we illustrate that miR-25 expression level modulated oxidative/nitrative stress and consequently neurological dysfunction by activating NADPH oxidase via phosphorylation of PKC-α accompanied by upregulating AGE–RAGE interaction.

Materials and methods
Animals
In this study, 8-week-old adult male BALB/c mice and db/db diabetic mice (SLAC Laboratory Animal) were maintained on a 12-h/12-h light/dark cycle (the light had been shining from 8:00 a.m. to 8:00 p.m.) with ad libitum access to normal chow and water. Blood glucose concentrations were measured from the tail vein using the glucose assay kit (Abcam, Cambridge, England). All experimental procedures were approved by the animal ethics review board of Second Affiliated Hospital of Harbin Medical University according to the 'Principles of Laboratory Animal Care' (National Institutes of Health Publications, No. 80–23, revised 1978).

Primary Schwann cell cultures
Schwann cells (SCs) were isolated and cultured according to a previous report [21]. Adult mice were killed and sciatic nerves were dissected out, stripped, and cultured in DMEM/F12 (1 : 1) medium (Gibco, Carlsbad, California, USA) supplemented with 20% fetal bovine serum, 2 µg/ml bovine pituitary extract (Gibco), 100 µg/ml streptomycin, and 100 units/ml penicillin at 37°C in a 5% humidified CO_2 atmosphere. The medium was changed every other day. After 1 week, the sciatic nerves were cut into pieces and digested with 0.25% trypsin and 0.1% collagenase II for 30 min at 37°C. Then the tissues were triturated, washed, and resuspended in culturing medium. Cells were dispersed into 35-mm culture dishes and transferred into poly-L-lysine-coated dishes after 30 min. Three days later, the cells were digested with 0.25% trypsin. When a majority of SCs detach, add DMEM/F12 (1 : 1) medium containing 20% fetal bovine serum to stop digestion and collect the detached cells. Thereafter, the cells were seeded into poly-L-lysine-coated six-well plates or 18-mm coverslips at a density of 2×10^5 cells/ml. The cells were cultured in the aforementioned medium supplemented with different concentrations of insulin and harvested after 72 h.

Reactive oxygen species assays
ROS level was measured with the Reactive Oxygen Species Assay Kit (Beyotime, Beijing, China) according to the manufacturer's instruction. In brief, SCs were transfected and incubated with dichloro-dihydro-fluorescein diacetate at 10 uM for 20 min at 37°C. Cells were washed with culture medium three times and the dichloro-dihydro-fluorescein diacetate-loaded cells were treated with the desired oxidant or antioxidant. The intensity of fluorescence was analyzed by flow cytometry analysis using excitation and emission wavelengths of 480 and 530 nm, respectively. Nontreated cells were used as control and the percentage increase in fluorescence was calculated by the formula $[(F_t - F_c)/F_c] \times 100\%$, where F_t = fluorescence of test samples and F_c = fluorescence of control samples.

Measurements of NADPH oxidase activity
NADPH oxidase activity was determined by measurement of O_2 production in sciatic nerves or cell homogenates as described [22]. Samples were treated with NADPH (100 µM) for 30 min before treatment with dihydroethidium (DHE, 10 µM) for 30 min at room temperature. Dihydroethidium intensity was measured at 518-nm excitation and 605-nm emission wavelengths, respectively.

Protein kinase C activity assay
Sciatic nerves were isolated and homogenized in ice-cold buffer A (20 mM Tris-HCl, pH 7.5; 2 mM EDTA; 10 mM EGTA; and 0.25 M sucrose) containing complete protease (Roche Diagnostics, Basel, Switzerland) and phosphatase inhibitors (Sigma, St. Louis, Missouri, USA). The homogenates were centrifuged at $1000\,g$ for 10 min. The supernatants were then centrifuged at $10\,000\,g$ at 4°C for 20 min. The supernatants were then ultracentrifuged at $100\,000\,g$ for 1 h at 4°C. This supernatant was retained as the cytosolic fraction, and the pellet was resuspended in buffer B (buffer A with 1% Triton X-100) and ultracentrifuged at $100\,000\,g$ for 1 h at 4°C. This supernatant was retained as the membranous fraction [23]. Membrane and cytosolic fractions were assayed for PKC activity using the StressXpress PKC Kinase Activity Assay Kit (EKS-420A; Stressgen Bioreagents, Victoria, Canada), as described previously [24].

Carboxymethyllysine enzyme-linked immunosorbent assay
The concentrations of carboxymethyllysine, an AGE, in serum and cytosolic extracts were assessed by an in-house indirect enzyme-linked immunosorbent assay [24]. Samples (1 : 10 000–1 : 20 000 dilution for serum and 1 : 1000 dilution for tissues) or standard were diluted in 50 mM carbonate buffer (pH: 9.6). Results are expressed in nmol per mol per lysine per mg protein as compared with a standard, measured by gas chromatography–mass spectrometry [24].

Flow cytometric analysis of surface receptor for advanced glycation endproducts expression on primary Schwann cells
Primary SCs were cultured for 7 days before performing the test. Cells were collected, washed in sterile PBS, and

centrifuged at 1000 rpm for 5 min and counted with a hemocytometer. An aliquot of 5×10^5 cells in each tube was incubated in 15 μl of goat anti-RAGE antibody (1 : 100 dilution Santa; Cruz Biotechnology, Santa Cruz, California, USA) or isotopic control at room temperature in the dark for 30 min. Cells were then rinsed with washing buffer (PBS with 2.5% fetal bovine serum and 0.01% NaN$_3$) three times and incubated in fluorescein isothiocyanate-conjugated rabbit antigoat IgG F(ab')$_2$ (1 : 100, Chemicon International, Temecula, California, USA) at room temperature for 30 min in the dark. The cells were rinsed again with washing buffer and subjected to FACS analysis. A minimum of 10 000 cells were analyzed on FACs Calibur (BD Biosciences, Lane Cove, Australia) equipped with the WinMDI 2.8 software (Scripps Institute, La Jolla, California, USA). RAGE-positive cells were gated and quantified relative to the isotopic controls.

Quantitative real-time PCR

Total RNA was extracted using TRIzol Reagent (Life Technologies, Carlsbad, California, USA) and digested with DNase (DNA-free; Life Technologies). A measure of 1 μg of total RNA was reverse transcribed to cDNA using the QuantiTect Reverse Transcription Kit (Qiagen, Düsseldorf, Germany). Real-time PCR was performed using the Applied Biosystems StepOne Real-time PCR System with SYBR Green PCR Master Mix (Applied Biosystems, Carlsbad, California, USA) according to the manufacturer's protocol. PCR conditions were 15 min at 95°C, followed by 45 cycles of 15 s at 95°C and 30 s at 60°C. The relative quantification method was used for the estimation of target mRNA expression according to the manufacturer's protocol. All measurements were performed in duplicate. GAPDH mRNA or U6 snRNA was used to normalize the relative expression levels of target mRNAs.

Western blotting

Western blotting was performed as described previously. Equal amounts of protein were separated on 10% SDS-PAGE gels and transblotted onto polyvinylidene difluoride membranes (GE Healthcare, Chicago, Illinois, USA). After blocking with 5% skim milk, membranes were incubated with the indicated primary antibody (Nox4 1 : 1000, PKC-α 1 : 1000, GAPDH 1 : 5000, β-actin 1 : 5000; Cell Signaling Technology, Danvers, Massachusetts, USA). After incubation with appropriate HRP-conjugated

secondary antibodies (1 : 4000; Cell Signaling Technology), the blots were developed using Pierce ECL Western Blotting Substrate Plus (Cell Signaling Technology, Danvers, Massachusetts, USA).

Delivery of miR-25 precursor or inhibitor into primary Schwann cells

Vector express miR-25 precursor driven by the cytomegalovirus promoter and vector expressing miR-25 inhibitor driven by the U6 promoter were purchased from GeneCopoeia and amplified. Primary SCs were cultured in six-well plates to 80% confluency and transfected with miR-25 precursor or inhibitor expressing vectors with Lipofectamine 3000 (Invitrogen, Carlsbad, California, USA) according to the manufacturer's instruction. At 48 h after transfection, the cells were collected for desired experiments.

Statistical analyses

Multiple groups were compared using analysis of variance (one way or two way) and least significant difference test. Unpaired *t*-tests were used for two-group comparisons. The tests were two-tailed and considered significant when *P* value less than 0.05. All data are presented as mean ± SEM.

Results

miR-25 and reactive oxygen species level changes in response to high glucose in diabetic mice

As shown in Table 1, in db/db mice, random-fed blood glucose levels were significantly higher compared with the wt mice, and were markedly increased over time. It is well documented that ROS could induce and promote pathological changes during the processes of multiple neurodegenerative diseases and diabetic peripheral neuropathy. To study the effects of ROS in DN, we first investigated the ROS level in sciatic nerves of db/db mice. As shown in Fig. 1a (the statistical results: $t = 7.283$, $P < 0.002$), we found increased resting ROS level in diabetic model mice compared with wt control, indicating that change of glucose levels could alter cellular oxidative stress. In order to cope with the high reactivity and toxicity of ROS *in vivo*, a crowd of antioxidant enzyme systems are evolved to scavenge mtROS as soon as they are generated [25]. Decreased expression levels of ROS detoxifying enzymes such as superoxidedismutase (Sod1), catalase (Cat), and glutathione peroxidase1 (Gpx1) were observed in diabetic mice in accordance with increased ROS levels (Fig. 1b, the statistical results are as follows: $t = 11.769$, 6.595, 5.126; $P < 0.001$, 0.003, 0.007). In addition, we found that NADPH oxidase activity (Fig. 1c, the statistical results: $t = 14.074$; $P < 0.001$), Nox4 mRNA (Fig. 1d, the statistical results: $t = 11.879$; $P < 0.001$), and protein levels (Fig. 1e, f, the statistical results: $t = 3.559$; $P < 0.024$) were significantly increased in sciatic nerves from diabetic mice. The accumulation of Nox4, an inflammation-promoting factor, was reported to trigger excess ROS production. Together, these data

Table 1 Changes in random-fed blood glucose level in wild-type, db/db mice

	4 weeks	6 weeks	8 weeks	12 weeks	24 weeks
Wt (mg/dl)	165.5 ± 12.4	170.8 ± 13.6	179.9 ± 14.5	173.7 ± 14.3	163 ± 12.6
db/db (mg/dl)	371 ± 24.9	463.3 ± 32.7	557.8 ± 40.5	736.9 ± 60.5	713 ± 53.2

Fig. 1
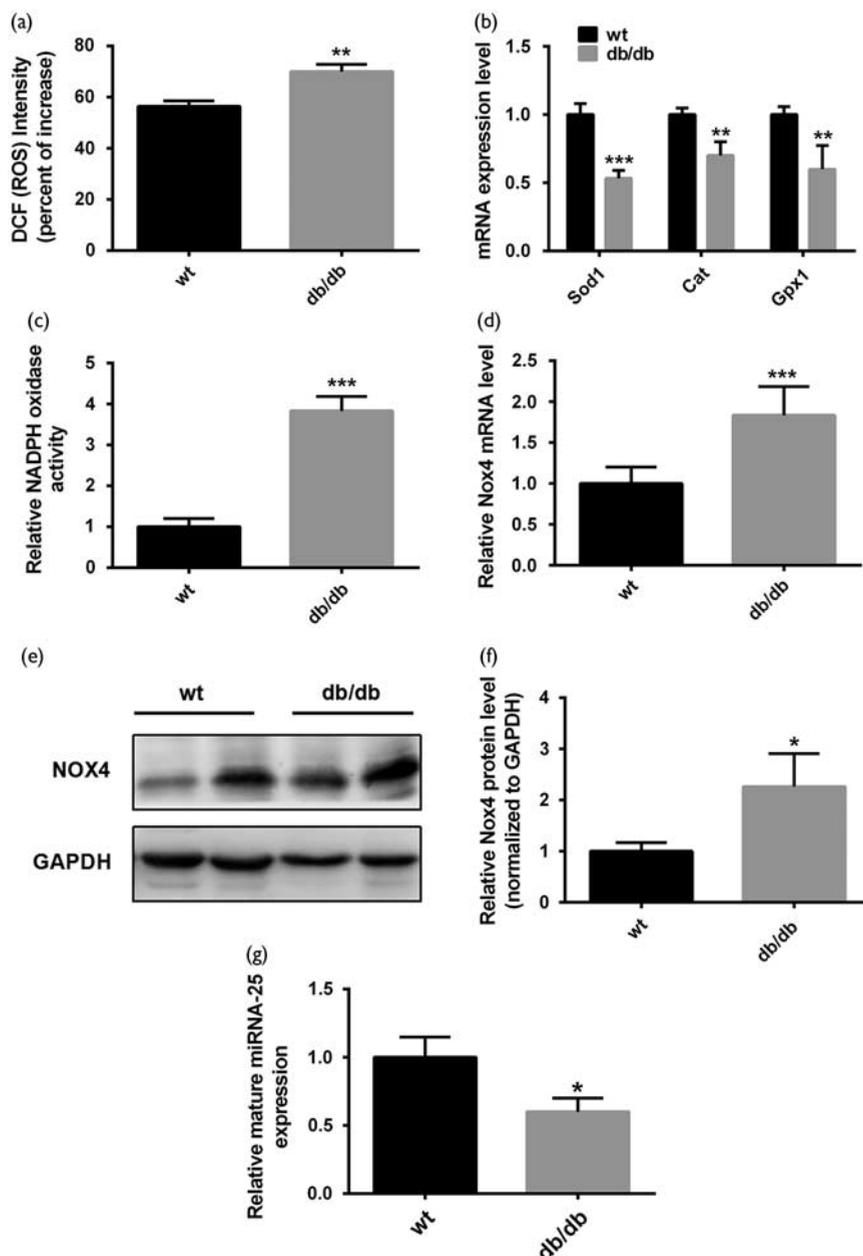
Increased ROS and Nox4 levels in sciatic nerves from diabetic mice. (a) Increased cellular ROS level determined by flow cytometry. DCF was a fluorescent indicator of ROS. (b) Decreased anti-ROS gene expression in sciatic nerves from diabetic mice determined by RT-qPCR. (c) NADPH oxidase activity in sciatic nerves from wt and diabetic mice. (d) Relative mRNA levels of Nox4 detected by RT-qPCR in sciatic nerves from wt and diabetic mice. (e) Nox4 protein level in sciatic nerves from wt and diabetic mice. (f) Quantitative statistics summarized data for the protein level of Nox4. (g) The level of miR-25 in sciatic nerves from wt and diabetic mice are detected by RT-qPCR. All quantitative data are presented as means ± SD of three independent experiments. DCF, dichloro-dihydro-fluorescein; ROS, reactive oxygen species; RT, reverse transcription. *$P < 0.05$; **$P < 0.01$; ***$P < 0.001$.

demonstrated that the mitochondrial dysfunction induced by high glucose and dysregulated metabolism in diabetic mice caused sustained ROS imbalance accompanied with increased Nox4 and NADPH oxidase activity, which was sufficient to exacerbate SCs damage of sciatic nerves. It was reported that miR-25 directly targeted 3′ untranslated region of Nox4 mRNA and modulated its abundance in the urinary system of diabetic rats. To investigate whether miR-25 is involved in the pathogenesis of DN, we examined miR-25 expression level and found that miR-25 was significantly reduced in sciatic nerves of diabetic mice (Fig. 1g, the statistical results: $t = 3.843$; $P < 0.0184$). This result suggested that miR-25 might be involved in the upregulation of ROS and Nox4 during the progress of DN.

Effects of miR-25 silence and overexpression on NADPH activity and Nox4 levels

To further determine whether miR-25 contributes to the dysregulation of ROS and Nox4 level in SCs of diabetic mice, miR-25 inhibitor and precursor expressing vector were used to study the effects of loss and gain of function. We found that miR-25 inhibitor transfection increased both ROS level and NADPH activity in SCs from diabetic mice. In contrast, miR-25 precursor-transfected diabetic mouse SCs exhibited decreased ROS level and NADPH activity (Fig. 2a, b, the statistical results are as follows: $F(3,8) = 307.634, 28.354; P < 0.001, 0.001$). Meanwhile, miR-25 silence markedly increased Nox4 mRNA levels in SCs from diabetic mice and reduced Nox4 mRNA expression in SCs from diabetic mice with miR-25 overexpression (Fig. 2c, the statistical

results: $F(3,8) = 18.392; P < 0.001$). We further found that Nox4 protein was also changed with the same tendency (Fig. 2d, e, the statistical results: $F(3,8) = 18.976; P < 0.001$). Together, these results indicated that miR-25 abundance may contribute to the dysregulation of ROS state and Nox4 level in diabetic mice.

## Superoxide generation and activation of protein kinase C-α in sciatic nerves are regulated by miR-25.

PKC-α was reported to play a role downstream of RAGE during oxidative stress. Consistent with previous reports, we found increased membranous PKC-α activity (phosphorylated) in SCs isolated from diabetic mice compared with wt control, which could be partially rescued by overexpression of miR-25 precursor (Fig. 3a, the statistical results: $F(4,10) = 29.354; P < 0.001$). The effect of

Fig. 2
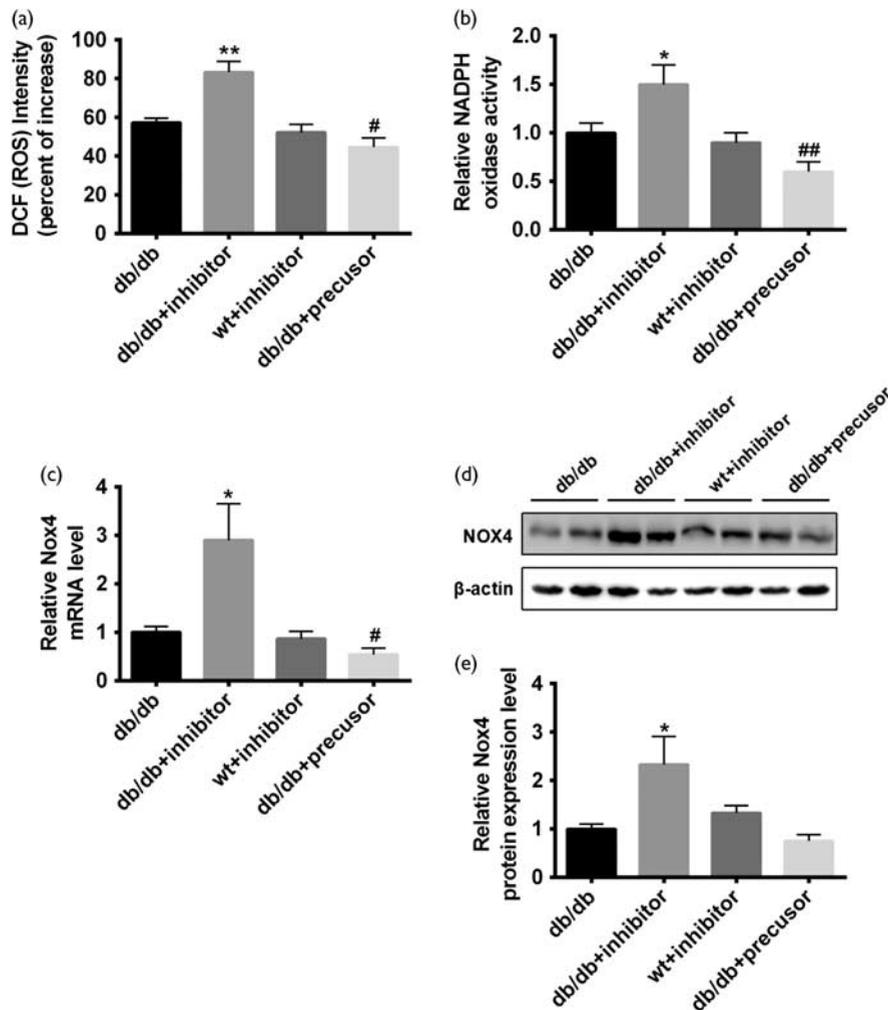
Effects of miR-25 inhibitor and miR-25 precursor treatments on the expression of NADPH and Nox4 levels in sciatic nerves. (a) ROS levels in sciatic nerves from wt and diabetic mice under miR-25 silencing or overexpression. (b) NADPH oxidase activity in SCs treated with miR-25 inhibitor or precursor-treated SCs. (c) Relative mRNA levels of Nox4 in treated SCs. (d) Nox4 protein levels in response to different treated SCs. (e) Quantitative statistics analysis of Nox4 protein level. All quantitative data are presented as means ± SD of three independent experiments. DCF, dichloro-dihydro-fluorescein; ROS, reactive oxygen species; RT, reverse transcription. *$P < 0.05$; **$P < 0.01$; #$P < 0.05$; ##$P < 0.01$.

Fig. 3
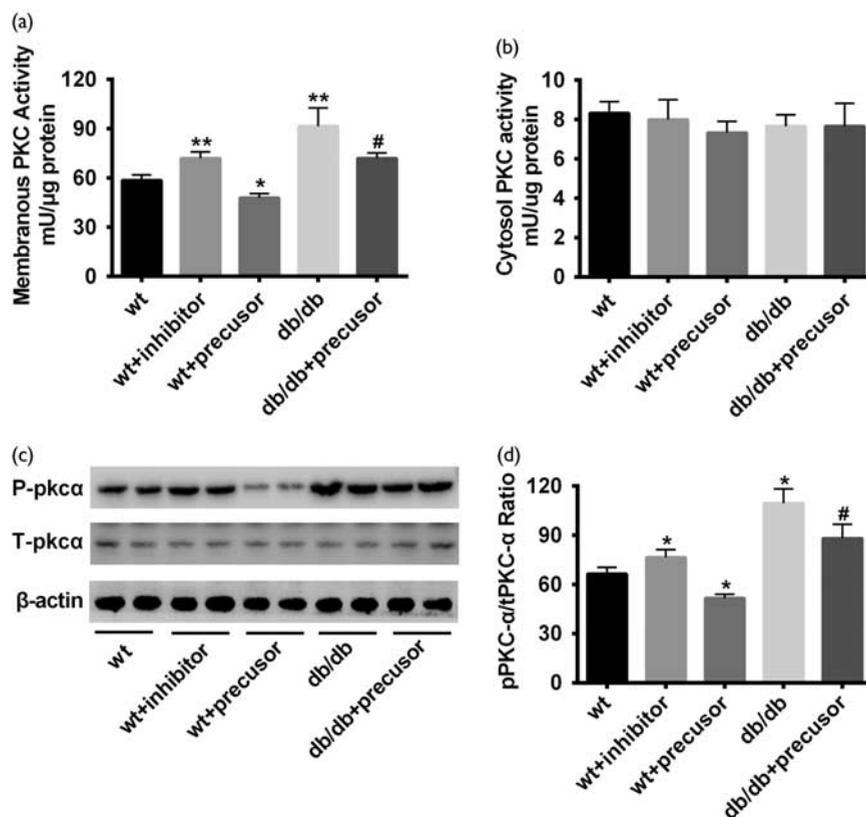
Activation of the phosphorylation of PKC-α is regulated by miR-25 expression level. (a) Membranous PKC activity by ELISA analysis. (b) Cytosolic PKC activity by ELISA analysis. (c) Representative Western blot result for pPKC-α (82 kDa) and tPKC-α (80 kDa) in sciatic nerves. (d) Quantification of Western blot for pPKC-α (82 kDa) and pPKC-α (80 kDa). All quantitative data are presented in means ± SD of three independent experiments. ELISA, enzyme-linked immunosorbent assay; PKC, protein kinase C. *$P < 0.05$; **$P < 0.01$; #$P < 0.05$.

miR-25 on PKC-α activity was also confirmed in SCs isolated from wt mice as treatment of miR-25 inhibitor increased PKC-α activity, whereas miR-25 precursor decreased PKC-α activity. There were no apparent activity changes of PKC-α among the cytosolic samples of either diabetic mice or wt control (Fig. 3b, the statistical results: $F(4,10) = 0.581$; $P > 0.683$). The ratio of phosphorylated PKC-α (pPKC-α) to total PKC-α (tPKC-α) is an important indicator of PKC-α activity. As shown in Fig. 3c, D (the statistical results: $F(4,10) = 77.485$; $P < 0.001$), we found that miR-25 overexpression reduced pPKC-α/tPKC-α ratio in primary SCs from wt and diabetic mice exposed to high glucose compared with controls. In contrast, miR-25 inhibition significantly elevated pPKC-α/tPKC-α ratio in primary SCs, which was also the case for diabetic nerves.

Knockdown of miR-25 in primary Schwann cells generates cytosolic inflammation via the advanced glycation endproducts–receptor for advanced glycation endproducts pathway

Previous studies showed that, in diabetic renal disease, the ratio of phosphorylated PKC-α to total PKC-α was increased with AGE exposure, suggesting that the activation of NADPH oxidase via phosphorylation of PKC-α is downstream of the AGE–RAGE interaction [26]. During DN development, we confirmed that high glucose exposure elevated phosphorylated PKC-α to total PKC-α ratio in primary SCs, and the change is more evident with the cells isolated from diabetic mice than that of controls. Thereafter, this PKC-α phosphorylation significantly induces NADPH oxidase activity in diabetic mice. Specifically, the AGE status, as represented by the concentration of carboxymethyllysine secreted into cell culture media and in SCs, was increased when treated with miR-25 inhibitor as compared with controls (Fig. 4a, b, the statistical results are as follows: $F(4,10) = 46.953, 43.259$; $P < 0.001, 0.001$). The AGE elevation trend was attenuated by treatment with miR-25 precursor transfection in SCs from both wt and diabetic mice. After miR-25 inhibitor transfection, cell surface expression of RAGE was increased in SCs from diabetic mice compared with control cells (Fig. 4e). MiR-25 precursor overexpression attenuated the incensement of RAGE expression as well. Cytosolic ROS was higher in primary SCs treated with miR-25 inhibitor compared with controls (Fig. 2a).

Fig. 4
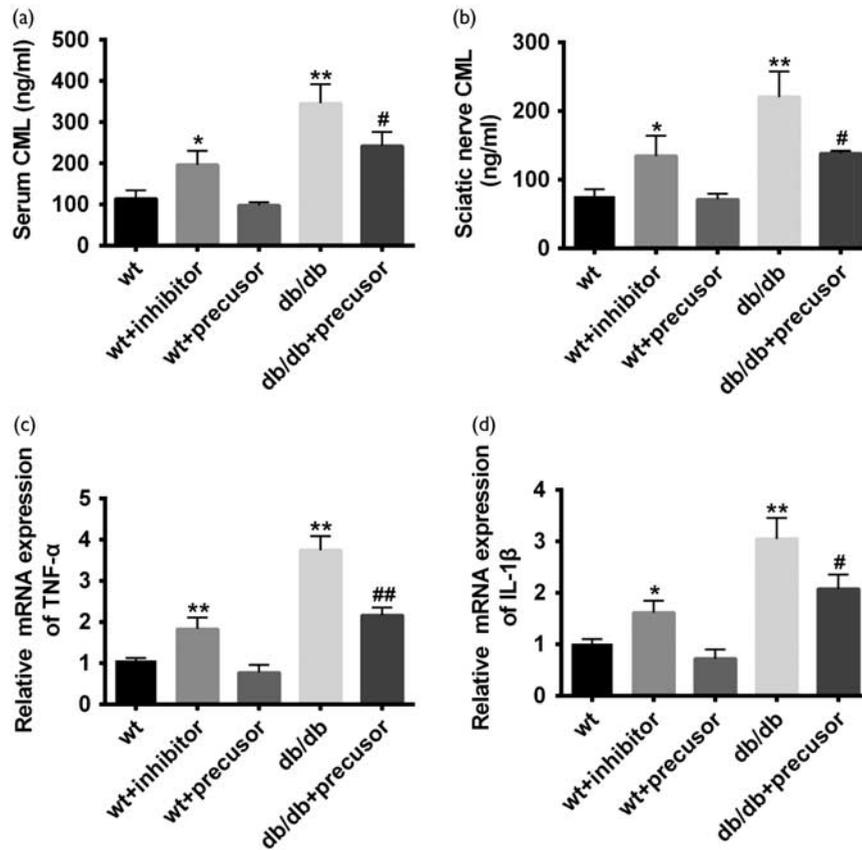
The accumulation of circulating and tissue AGEs and RAGE are induced by miR-25 silence. (a) Serum carboxymethyllysine concentrations are determined by ELISA analysis. (b) The detection of carboxymethyllysine in sciatic nerve by ELISA. (c, d) RT-qPCR analysis was used to analyze the expression levels of the inflammatory markers TNFα and IL-1β. (e) Flow cytometric analysis of cell surface. RAGE in various groups. All quantitative data are presented in means ± SD of three independent experiments. AGE, advanced glycation endproduct; ELISA, enzyme-linked immunosorbent assay; IL-1β, interleukin-1β; RAGE, receptor for advanced glycation endproduct; TNFα, tumor necrosis factor-α. $*P < 0.05$; $**P < 0.01$; $^{\#}P < 0.05$; $^{\#\#}P < 0.01$.

We further investigated the expression patterns of inflammatory factors tumor necrosis factor-α (TNFα) and interleukin (IL)-1β, two important mediators of neuropathic pain, after the transfection of miR-25 inhibitor or precursor in primary SCs. Both TNFα and IL-1β were significantly increased after miR-25 silencing in SCs; accordingly, miR-25 overexpression markedly decreased TNFα and IL-1β expression (Fig. 4c, d, the statistical results are as follows: $F(4,10) = 116.123, 56.293; P < 0.001, 0.001$), indicating that miR-25 may be involved in the regulation of neuropathic pain.

Together, these results revealed that miR-25 was a key molecule regulating Nox4 expression and subsequently stimulating neuropathic inflammation, leading to neuron damage, nerve endothelial injury, and neuropathic pain.

Discussion

Microvascular complications, including retinopathy, nephropathy, and neuropathy accompanied with neuropathic pain, are most common among diabetes patients

[27,28]. These complications are caused by various pathological factors and pathways, which are closely linked to increased mitochondrial oxidant stress and NADPH oxidase activation [14,15]. Although ROS such as superoxide anions may be short lived, their effects can be long lasting due to subsequent activation of multiple downstream signaling pathways. ROS also co-operate with reactive nitrogen species such as nitrotyrosine and peroxynitrite to further enhance diabetes-induced cellular dysfunction [29]. Hyperglycemia and consequent increases in oxidant stress, AGEs, PKC, and mitogen-activated protein kinases lead to increased activation of nuclear factor-κB, a proinflammatory transcription factor, which promotes the expression of key inflammatory genes [16,17]. Inflammation plays a major role in several diabetic complications, and contributes to β-cell failure in T1D and insulin resistance in T2D. Diabetes-related oxidant stress, including mitochondrial oxidant stress and other cellular stresses, are important pathogenic factors for diabetic complications, and genes Nox4 and NRF2 are found to be involved in downstream signaling

pathways [30–32]. Seven members of the Nox family, Nox1 to Nox5, DUOX1, and DUOX2, are identified in mammals. Nox4 is most closely related to diabetic complications. It was reported that reduced expression of Nox2, Nox4, and caspase-3 in bupivacaine-treated diabetic rats led to less ROS production, cell apoptosis, and nerve injury [33]. In diabetic nephropathy, Nox4 was found to be prominently expressed in the microvascular endothelium as a major subunit of NADPH oxidase, which mediated O_2 production [34].

Recent findings revealed critical functions of specific miRNAs in regulating genes relevant to diabetic nephropathy [35,36], but little is known whether miRNAs would regulate the NADPH oxidase pathway in DN. Therefore, this study was aimed to highlight functions of miRNAs and their relationships to redox signaling molecules during DN pathogenesis. We focused on miR-25, which is expressed in the kidney and peripheral neural stem/progenitor cells playing important physiologic and pathological roles. It was reported that miR-25 is sensitive to hypoxia and its expression was elevated under low oxygen circumstance, and further induced immunosuppression by directly inducing cGAS mRNA degradation [37]. Immunosuppression is a risk factor for tumor progression but, in contrast, may benefit patients with autoimmune diseases such as diabetes. As a matter of fact, the expression of miR-25 was found to be reduced in diabetic patients and administration of miR-25 antagomir in model mice induced diabetic changes, such as proteinuria, extracellular matrix accumulation, podocyte foot process effacement, and hypertension [38]. In the present study, we first investigated whether hyperglycemia regulates miR-25 expression in Sciatic nerves. We found that, in response to high glucose, miR-25 expression was significantly decreased in contrast to the incensement in ROS and Nox4 expression, suggesting a connection between miR-25 and Nox4 pathway, which was further confirmed with the syn-kinetic changes of Nox4 after miR-25 manipulation. Consistent with previous report [39], we also found increased phosphorylation of PKC-α, which could be rescued by overexpression of miR-25 precursor or aggravate by miR-25 inhibition, suggesting that miR-25 exerted function upstream of PKC-α. Last, we confirmed PKC-α activity changes during modulation of miR-25 in isolated SCs and determined the activation of inflammation pathway of AGE–RAGE when miR-25 was dysfunctional.

To sum up, our findings provide relative complete view of how miR-25 dysregulation contributes to oxidative stress and finally DN in diabetic mice, suggesting that miR-25 could be a potential diagnostic and therapeutic target for complications of diabetes.

Acknowledgements

References
1   Patterson C, Guariguata L, Dahlquist G, Soltesz G, Ogle G, Silink M. Diabetes in the young – a global view and worldwide estimates of numbers of children with type 1 diabetes. *Diabetes Res Clin Pract* 2014; **103**:161–175.
2   Guariguata L. By the numbers: new estimates from the IDF Diabetes Atlas Update for 2012. *Diabetes Res Clin Pract* 2012; **98**:524–525.
3   Huizinga MM, Roumie CL, Elasy TA, Murff HJ, Greevy R, Liu X, *et al.* Changing incident diabetes regimens: a Veterans Administration Cohort Study from 2000 to 2005. *Diabetes Care* 2007; **30**:e85.
4   Vinik AI, Mehrabyan A. Diabetic neuropathies. *Med Clin North Am* 2004; **88**:947–999.
5   Cameron NE, Cotter MA. Potential therapeutic approaches to the treatment or prevention of diabetic neuropathy: evidence from experimental studies. *Diabet Med* 1993; **10**:593–605.
6   Nagamatsu M, Nickander KK, Schmelzer JD, Raya A, Wittrock DA, Tritschler H, *et al.* Lipoic acid improves nerve blood flow, reduces oxidative stress, and improves distal nerve conduction in experimental diabetic neuropathy. *Diabetes Care* 1995; **18**:1160–1167.
7   Obrosova IG, van Huysen C, Fathallah L, Cao XC, Greene DA, Stevens MJ. An aldose reductase inhibitor reverses early diabetes-induced changes in peripheral nerve function, metabolism, and antioxidative defense. *FASEB J* 2002; **16**:123–125.
8   Schmeichel AM, Schmelzer JD, Low PA. Oxidative injury and apoptosis of dorsal root ganglion neurons in chronic experimental diabetic neuropathy. *Diabetes* 2003; **52**:165–171.
9   Stevens MJ, Obrosova I, Cao X, van Huysen C, Greene DA. Effects of DL-alpha-lipoic acid on peripheral nerve conduction, blood flow, energy metabolism, and oxidative stress in experimental diabetic neuropathy. *Diabetes* 2000; **49**:1006–1015.
10 Tomlinson DR. Future prevention and treatment of diabetic neuropathy. *Diabetes Metab* 1998; **24 (Suppl 3)**:79–83.
11 Vincent AM, Brownlee M, Russell JW. Oxidative stress and programmed cell death in diabetic neuropathy. *Ann N Y Acad Sci* 2002; **959**:368–383.
12 Vincent AM, Feldman EL. New insights into the mechanisms of diabetic neuropathy. *Rev Endocr Metab Disord* 2004; **5**:227–236.
13 Brownlee M. Biochemistry and molecular cell biology of diabetic complications. *Nature* 2001; **414**:813–820.
14 Brownlee M. The pathobiology of diabetic complications: a unifying mechanism. *Diabetes* 2005; **54**:1615–1625.
15 Devaraj S, Dasu MR, Jialal I. Diabetes is a proinflammatory state: a translational perspective. *Expert Rev Endocrinol Metab* 2010; **5**:19–28.
16 Devaraj S, Glaser N, Griffen S, Wang-Polagruto J, Miguelino E, Jialal I. Increased monocytic activity and biomarkers of inflammation in patients with type 1 diabetes. *Diabetes* 2006; **55**:774–779.
17 Schmidt AM, Hori O, Brett J, Yan SD, Wautier JL, Stern D. Cellular receptors for advanced glycation end products. Implications for induction of oxidant stress and cellular dysfunction in the pathogenesis of vascular lesions. *Arterioscler Thromb* 1994; **14**:1521–1528.
18 Shanmugam N, Gaw Gonzalo IT, Natarajan R. Molecular mechanisms of high glucose-induced cyclooxygenase-2 expression in monocytes. *Diabetes* 2004; **53**:795–802.
19 Fu Y, Zhang Y, Wang Z, Wang L, Wei X, Zhang B, *et al.* Regulation of NADPH oxidase activity is associated with miRNA-25-mediated NOX4 expression in experimental diabetic nephropathy. *Am J Nephrol* 2010; **32**:581–589.
20 Meza-Sosa KF, Pedraza-Alva G, Perez-Martinez L. microRNAs: key triggers of neuronal cell fate. *Front Cell Neurosci* 2014; **8**:175.
21 Tao Y. Isolation and culture of Schwann cells. *Methods Mol Biol* 2013; **1018**:93–104.
22 Wang Z, Wei X, Zhang Y, Ma X, Li B, Zhang S, *et al.* NADPH oxidase-derived ROS contributes to upregulation of TRPC6 expression in puromycin aminonucleoside-induced podocyte injury. *Cell Physiol Biochem* 2009; **24**:619–626.
23 Baines CP, Zhang J, Wang GW, Zheng YT, Xiu JX, Cardwell EM, *et al.* Mitochondrial PKCepsilon and MAPK form signaling modules in the murine heart: enhanced mitochondrial PKCepsilon-MAPK interactions and differential MAPK activation in PKCepsilon-induced cardioprotection. *Circ Res* 2002; **90**:390–397.
24 Coughlan MT, Thallas-Bonke V, Pete J, Long DM, Gasser A, Tong DC, *et al.* Combination therapy with the advanced glycation end product cross-link breaker, alagebrium, and angiotensin converting enzyme inhibitors in diabetes: synergy or redundancy? *Endocrinology* 2007; **148**:886–895.

25 Li X, Fang P, Mai J, Choi ET, Wang H, Yang XF. Targeting mitochondrial reactive oxygen species as novel therapy for inflammatory diseases and cancers. *J Hematol Oncol* 2013; **6**:19.

26 Thallas-Bonke V, Thorpe SR, Coughlan MT, Fukami K, Yap FY, Sourris KC, *et al.* Inhibition of NADPH oxidase prevents advanced glycation end product-mediated damage in diabetic nephropathy through a protein kinase C-alpha-dependent pathway. *Diabetes* 2008; **57**:460–469.

27 Beckman JA, Creager MA, Libby P. Diabetes and atherosclerosis: epidemiology, pathophysiology, and management. *JAMA* 2002; **287**:2570–2581.

28 He Z, King GL. Microvascular complications of diabetes. *Endocrinol Metab Clin North Am* 2004; **33**:215–238.

29 Zou MH, Cohen R, Ullrich V. Peroxynitrite and vascular endothelial dysfunction in diabetes mellitus. *Endothelium* 2004; **11**:89–97.

30 Babelova A, Avaniadi D, Jung O, Fork C, Beckmann J, Kosowski J, *et al.* Role of Nox4 in murine models of kidney disease. *Free Radic Biol Med* 2012; **53**:842–853.

31 Kaspar JW, Niture SK, Jaiswal AK. Nrf2:INrf2 (Keap1) signaling in oxidative stress. *Free Radic Biol Med* 2009; **47**:1304–1309.

32 Lowell BB, Shulman GI. Mitochondrial dysfunction and type 2 diabetes. *Science* 2005; **307**:384–387.

33 Ji ZH, Liu ZJ, Liu ZT, Zhao W, Williams BA, Zhang HF, *et al.* Diphenyleneiodonium mitigates bupivacaine-induced sciatic nerve damage in a diabetic neuropathy rat model by attenuating oxidative stress. *Anesth Analg* 2017; **125**:653–661.

34 Paravicini TM, Touyz RM. NADPH oxidases, reactive oxygen species, and hypertension: clinical implications and therapeutic possibilities. *Diabetes Care* 2008; **31** (**Suppl 2**):S170–S180.

35 Gill PS, Wilcox CS. NADPH oxidases in the kidney. *Antioxid Redox Signal* 2006; **8**:1597–1607.

36 Ryan BM, Robles AI, Harris CC. Genetic variation in microRNA networks: the implications for cancer research. *Nat Rev Cancer* 2010; **10**:389–402.

37 Wu MZ, Cheng WC, Chen SF, Nieh S, O'Connor C, Liu CL, *et al.* miR-25/93 mediates hypoxia-induced immunosuppression by repressing cGAS. *Nat Cell Biol* 2017; **19**:1286–1296.

38 Liu Y, Li H, Liu J, Han P, Li X, Bai H, *et al.* Variations in MicroRNA-25 expression influence the severity of diabetic kidney disease. *J Am Soc Nephrol* 2017; **28**:3627–3638.

39 Thallas-Bonke V, Lindschau C, Rizkalla B, Bach LA, Boner G, Meier M, *et al.* Attenuation of extracellular matrix accumulation in diabetic nephropathy by the advanced glycation end product cross-link breaker ALT-711 via a protein kinase C-alpha-dependent pathway. *Diabetes* 2004; **53**:2921–2930.